View metadata, citation and similar papers at core.ac.uk

brought to you by CORE

provided by Hiroshima University Institutional Repository

広島大学学術情報リポジトリ
Hiroshima University Institutional Repository

Title	Theoretical basis of SQUID-based artificial neurons
Author(s)	Katayama, Haruna; Fujii, Toshiyuki; Hatakenaka, Noriyuki
Citation	Journal of Applied Physics , 124 (15) : 152106
Issue Date	2018-09-25
DOI	10.1063/1.5037718
Self DOI	
URL	https://ir.lib.hiroshima-u.ac.jp/00049006
Right	This document is the Accepted Manuscript version of a Published Work that appeared in final form in Journal of Applied Physics, copyright © AIP Publishing after peer review and technical editing by the publisher. To access the final edited and published work see https://doi.org/10.1063/1.5037718. This is not the published version. Please cite only the published version. この論文は出版社版でありません。引用の際には出版社版をご確認、ご利用ください。
Relation	

Hiroshima University Institutional Repository

Theoretical basis of SQUID-based artificial neurons

Haruna Katayama,[1] Toshiyuki Fujii,[2] and Noriyuki Hatakenaka[3, a)]
[1)] *Faculty of Integrated Arts and Sciences, Hiroshima University.*
[2)] *Department of Physics, Asahikawa Medical University.*
[3)] *Graduate School of Integrated Arts and Sciences, Hiroshima University.*

(Dated: 24 June 2018)

The physical basis of an artificial neuron is studied using a model that is based on the stochastic transition between two states in a double well potential. It is shown that the stochastic transition model generates an energy-defined sigmoid function acting as an activation (or transfer) function in neurons. The model is also applied to circuit neurons using superconducting quantum interference devices (SQUIDs) in artificial neural networks.

PACS numbers: 87.19.ll, 85.25.Dq, 07.05.Mh

I. INTRODUCTION

Artificial Intelligence (AI) is a rapidly growing indispensable technology that is driving both the scientific evolution and industrial progress in contemporary society inherent in complexity and uncertainty. The fundamental technology supporting AI is the Artificial Neural Network (ANN)[1] which is a biological nerve-inspired system. It is not programmed in the traditional way, but trained using historical data that represent the behaviour of a target system. This enables us to handle complicated problems on noisy and incomplete data in various fields like pattern recognition.

ANN is considerably simplified despite its complexity in the actual nervous system. It comprises many neuron elements arranged in the layered structure, which are interconnected to one another via synapse elements. There are different types of ANN that depends on the intended tasks. It is classified into feed-forward neural network and feed-back (or recurrent) neural network that considers the connectivity of the neurons in a network. The feed-forward ANN was the first and most simple type of artificial neural network devised. In this network, information flows in only one direction along the connecting pathways from the input layer via the hidden layers to the output layer as shown in Fig. 1. There is also no feedback loop in this network contrary to the recurrent network.

The artificial neuron is composed of synapses and a soma as shown in Fig. 2. It receives one or more individually weighted inputs that are produced at the synapses and sums them at a soma. An output is generated according to the activation function representing the neuron's *nonlinear* action potential. The activation functions are therefore the heart of the neuron. Among the various nonlinear functions, sigmoid function is the most suitable mathematical tool for learning algorithm based on the back-propagation scheme[2]. It is represented as

$$f(x) = \frac{1}{1+e^{-x}}. \tag{1}$$

This simplified model makes it possible to realize a scalable artificial neural network by VLSI technology based on the latest nanotechnology. In fact, ANN can be realized in various systems[3,4]. Among solid-state devices, a superconducting circuit is also a promising candidate

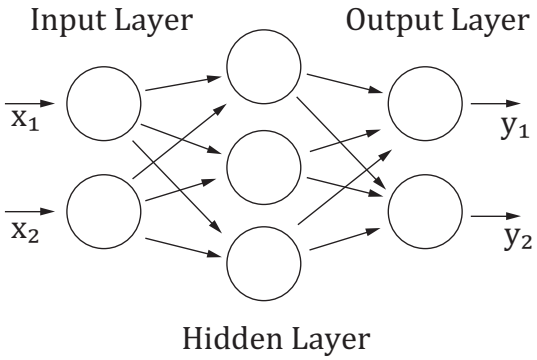

FIG. 1. A three-layered feed-forward neural network.

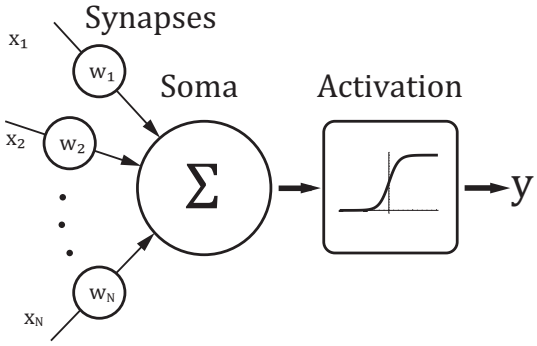

FIG. 2. Schematic diagram of an artificial neuron.

a)Electronic mail: noriyuki@hiroshima-u.ac.jp.

because of its ultra-high speed operation and ultra-low power consumption even though it is forced to operate at low temperatures. In particular, it is suitable for realizing threshold logic circuits using nonlinearity inherent in Josephson elements. In fact, ANN using Josephson elements has been proposed[5,6] in the early 90s, there have been successful implementations using different ways.[7–11]

In the previous studies, different types of activation functions in artificial neurons are employed to construct the superconducting artificial neural networks. For example, the two-stage coupled SQUID with a cascade connection produced a step-like function[9] and the rapid single flux quantum (RSFQ) comparator based on the statistical transition provided the error function similar to sigmoid function[10]. Interestingly, Yamanashi et. al., found the pseudo sigmoid function even in the RSFQ comparator[11]. However, there has been no existing system that can exactly generate sigmoid function for error back propagation learning algorithm. In addition, the theoretical basis of artificial neurons with sigmoid function has not been fully discussed.[12]

Hence in this paper, we present the physical basis of the sigmoid function acting as an activation function in neurons which are the building blocks of ANNs based on a typical two-state stochastic transition model. The model will then be used to analyze simplified SQUID-based artificial neurons.

II. PHYSICAL BASIS OF ARTIFICIAL NEURONS

Here we discuss the physical basis of sigmoid function generation. Let us consider the transition between two states as a nonlinear physical phenomenon that results to a binary function as shown in Fig. 3. The rate equation of this system is given as[13]

$$\frac{dp_L}{dt} = -\Gamma_{LR}p_L + \Gamma_{RL}p_R \tag{2}$$

$$\frac{dp_R}{dt} = -\Gamma_{RL}p_R + \Gamma_{LR}p_L \tag{3}$$

where the probability of finding a particle in the left (right) well is denoted by $p_{L(R)}$. Γ_{ij} stands for the transition rate from the i state to the j state. Since the conservation law for probability $(p_L + p_R = 1)$ based on $d(p_L + p_R)/dt = 0$, then these coupled equations are reduced to

$$\frac{dp_L}{dt} = -(\Gamma_{LR} + \Gamma_{RL})p_L + \Gamma_{RL}. \tag{4}$$

This can be analytically solved under the initial condition $p_L(0) = 1$,

$$p_L = \left(1 - \frac{\Gamma_{RL}}{\Gamma_{LR} + \Gamma_{RL}}\right) e^{-(\Gamma_{LR}+\Gamma_{RL})t} + \frac{\Gamma_{RL}}{\Gamma_{LR} + \Gamma_{RL}}. \tag{5}$$

Here, the relaxation time τ is defined as

$$\tau = \frac{1}{\Gamma_{LR} + \Gamma_{RL}} \tag{6}$$

which is a measure to estimate the time required to reach the equilibrium state any moment later. In equilibrium, Equation (5) is reduced to

$$p_L = \frac{\Gamma_{RL}}{\Gamma_{LR} + \Gamma_{RL}} = \frac{1}{1 + \Gamma_{LR}/\Gamma_{RL}}. \tag{7}$$

This is a fundamental formula based on stochastic transition model.

Here we employ the Arrhenius transition formula justified by the transition state theory[14,15] for the transition rate given as

$$\Gamma = \frac{\omega_0}{2\pi} e^{-\frac{\Delta U}{k_B T}} \tag{8}$$

where ΔU represents the barrier height as exemplified by $\Delta E_{L(R)}$ in Fig. 3. ω_0 is the angular frequency inside the metastable minimum while k_B and T are the Boltzmann constant and temperature, respectively. This yields the sigmoid function expressed by

$$p_L = \frac{1}{1 + e^{-\frac{\Delta E}{k_B T}}} \tag{9}$$

where ΔE is the energy difference between two states. This expression is no other than the basic formula for a neuron response in the Boltzmann machine[16] which is a type of stochastic recurrent neural network.

Here we note that the Boltzmann distribution imposed in the beginning of the Boltzmann machine is not assumed in the derivation of the basic equation (7). The obtained scheme is totally different from the Boltzmann machine. This allows us to extend neurons to the quantum-mechanical domain. In semiclassical regime, the transition rate by quantum tunneling[17] is roughly given by replacing $k_B T$ with $\hbar\omega$ in Eq. (8). In this way, the above generation scheme is made available for any system with stochastic transition processes. Therefore, this will serve as a guideline for designing sigmoid functions in any physical system.

Note that the obtained sigmoid function is a function of energy difference which is system dependent. This is good for energy defined neurons like in the Boltzmann machine. However, energy is generally not a suitable input variable. Therefore, it is necessary to confirm that this energy difference is proportional to the input variable when the sigmoid function is generated by using this transition scheme.

III. SQUID-BASED ARTIFICIAL NEURONS

Now let us apply the above transition scheme in generating the sigmoid function to artificial neurons based on

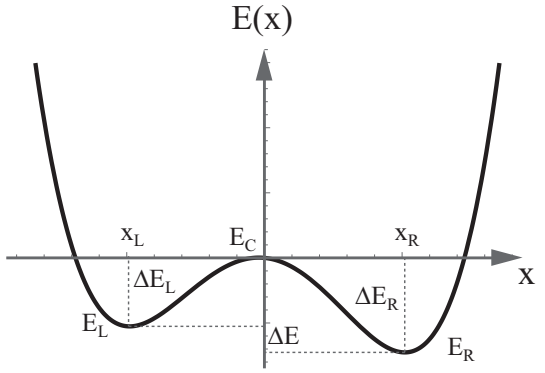

FIG. 3. Schematic diagram of double well potential.

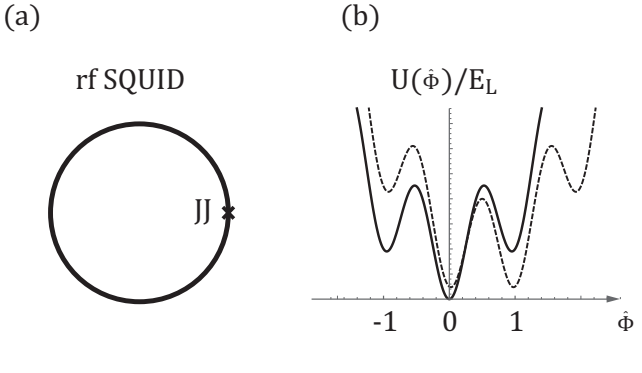

FIG. 4. (a) An rf SQUID and (b) its potential profile with $\hat{\Phi}_{ex} = 0$ (solid line) and $\hat{\Phi}_{ex} = 0.5$ (dotted line).

superconducting devices. As an artificial neuron, we consider the system known as an rf SQUID, which consists of a superconducting loop with the inductance L interrupted by a Josephson junction (JJ) as shown in Fig. 4 (a). The double SQUID-based ANN architecture has already been discussed by Chiarello et. al.[18] . The SQUID neuron responds in nonlinear way to the sum of the input magnetic fluxes applied to its loop. The SQUID state as an output is detected by the dc-SQUID arranged nearby. Unfortunately, there are no presented discussions on sigmoid function in their paper.

The potential energy of rf SQUID is given by

$$U(\hat{\Phi}) = E_L(\hat{\Phi} - \hat{\Phi}_{ex})^2 + E_J[1 - \cos(2\pi\hat{\Phi})] \qquad (10)$$

where $\hat{\Phi}$ and $\hat{\Phi}_{ex}$ are the magnetic flux through the superconducting ring and an externally applied magnetic flux respectively. These are normalized by the quantum unit of magnetic flux $\Phi_0 = h/2e$ where h is the Plank constant and e is an elementary electric charge. The first term represents the magnetic energy accumulated in the ring with $E_L = \Phi_0^2/2L$. On the other hand, the second term is the Josephson coupling energy given by $E_J = \hbar I_c/2e$ with I_c being the Josephson critical current.

Figure 4 (b) shows the potential profile as a function of $\hat{\Phi}$ with different applied magnetic flux values $\hat{\Phi}_{ex}$. The lowest two minima form a double well potential required to generate the sigmoid function discussed in the previous section.

Before we proceed in the discussion of the linearity of input signals in this system, we shall first consider the equilibrium state of the system which is an important assumption in a two-state transition state scheme. As discussed in the previous section, the time to reach the equilibrium state can be roughly estimated by the relaxation time τ. The assumption is not satisfied if the transition rate is small which is equivalent to a long relaxation time. The upper limit of the transition rate is given in the case of bias $\hat{\Phi}_{ex} = 0.5$ where the potential barrier is highest, roughly $2E_J$ and is expressed as

$$\tau \sim \frac{2\pi}{\omega_0} e^{\frac{2E_J}{k_B T}}. \qquad (11)$$

The attempt frequency ω_0 of the prefactor is given as

$$\omega_0 = \sqrt{\frac{d^2U/d\hat{\Phi}^2}{m}} \simeq \frac{1}{\hbar}\sqrt{8E_J E_c\left(1 + \frac{1}{\pi\beta_L}\right)} \qquad (12)$$

where m is the mass of the particle in the potential expressed as $\Phi_0^2 C$ in the case of SQUID. E_c is the charging energy defined as $e^2/2C$ with C being the junction capacitance. β_L is the dimensionless inductance parameter equivalent to $2\pi E_J/E_L$. This reduces to Josephson plasma frequency when $E_L = 0$ or equivalently $\beta_L = \infty$.

Now let us estimate the relaxation time using the typical junction parameters. At the fixed temperature ($T = 4.2$K), there are three junction parameters namely, E_J, E_c and E_L. In the case of classical Josephson junction, C is less than 10^{-12}F. On the other hand, E_L and E_J are restricted by the condition in the formation of a double well potential $2 < \beta_L$. Figure 5 shows the relaxation time as a function of the Josephson critical current in the case of $\beta_L = 2\pi$ as an example.

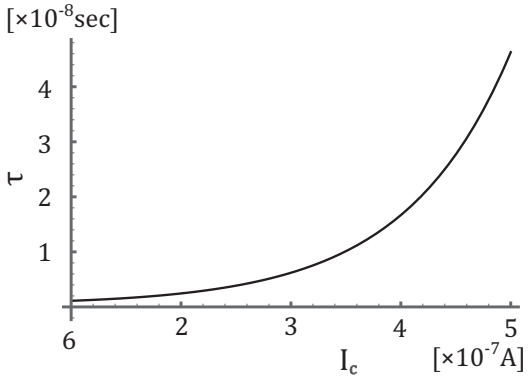

FIG. 5. The relaxation time τ as a function of the Josephson critical current I_c at $T = 4.2$K, $C = 1 \times 10^{-14}$F, and $\beta_L = 2\pi$.

Under these junction parameters, the relaxation time is measured in sub-micro seconds. This indicates that there are junction parameters satisfying the equilibrium condition. The relaxation time is extremely sensitive to the Josephson critical current, so careful handling of the junction parameters is necessary in the neuron design. In other words, the time to reach the equilibrium state becomes extremely large by only a few magnitudes than the Josephson critical current ($\tau \sim 10^{14}$ sec for $I_c \sim 5\mu$A).

Next, we show that the energy difference between two minima is proportional to the external magnetic flux. The energy difference is given as

$$\begin{aligned}\Delta E(\hat{\Phi}_{ex}) &= E(\hat{\Phi}_L) - E(\hat{\Phi}_R) \\ &= E_L[(\hat{\Phi}_R + \hat{\Phi}_L) - 2\hat{\Phi}_{ex}] \\ &\quad + 2E_J \sin(\pi(\hat{\Phi}_R+\hat{\Phi}_L)) \sin(\pi(\hat{\Phi}_R-\hat{\Phi}_L))\end{aligned} \tag{13}$$

where $\hat{\Phi}_{L(R)}$ is the magnetic flux giving the local minimum on the left (right) side of the double well potential and is given as solutions to the following equation determined from $dE/d\hat{\Phi} = 0$,

$$\sin(2\pi\hat{\Phi}) = -\frac{2}{\beta_L}(\hat{\Phi} - \hat{\Phi}_{ex}). \tag{14}$$

Unfortunately, $\hat{\Phi}_{L(R)}$ could hardly be solved analytically which called us to do neumerical methods. The numerical solutions of $\hat{\Phi}_{L(R)}$ for $\beta_L = 2\pi$ are shown in Fig. 5 (a).

In this figure both $\hat{\Phi}_L$ and $\hat{\Phi}_R$ can be well described as proportional to the external magnetic flux. In the case of $\beta_L = 2\pi$, these are fitted as

$$\hat{\Phi}_L = 0.04868\hat{\Phi}_{ex} - 0.00014 \tag{15}$$

$$\hat{\Phi}_R = 0.04868\hat{\Phi}_{ex} + 0.9512. \tag{16}$$

Suprisingly, it turns out that both have the same slope.

Within the range of the third order of external magnetic flux $O(\hat{\Phi}_{ex}^3)$, the slope can be approximated as follows;

$$\frac{\Delta\hat{\Phi}_{L(R)}}{\Delta\hat{\Phi}_{ex}} \simeq \frac{1}{1+\pi\beta_L}. \tag{17}$$

This approximated slope expression yields 0.0482 which is in a good agreement with the numerical value.

Moreover, we obtained the expression for $\Delta E/E_L$ in the linear form as

$$\Delta E(\hat{\Phi}_{ex})/E_L = a\hat{\Phi}_{ex} + b \tag{18}$$

where

$$a = \frac{2\pi\beta_L}{1+\pi\beta_L}[2(\hat{\Phi}_{R0} - \hat{\Phi}_{L0}) - 1] \tag{19}$$

$$\begin{aligned}b &= \pi\beta_L(1 - 2\hat{\Phi}_{R0}) \\ &\quad - (1-\pi\beta_L)(\hat{\Phi}_{R0} + \hat{\Phi}_{L0})(\hat{\Phi}_{R0} - \hat{\Phi}_{L0})\end{aligned} \tag{20}$$

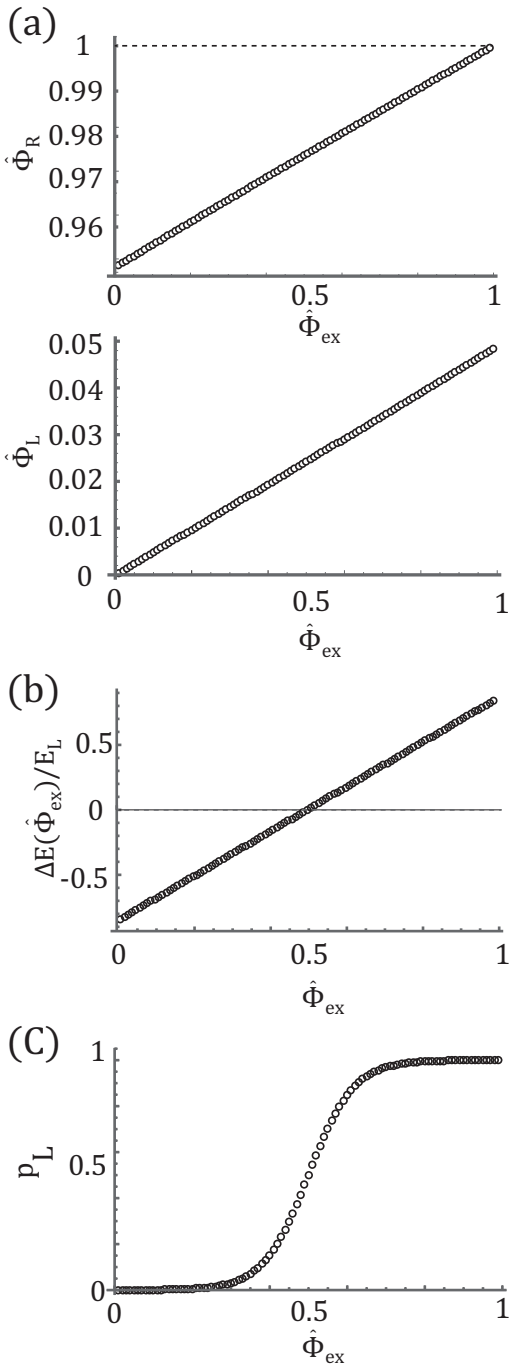

FIG. 6. Numerical Results (a) $\hat{\Phi}_{L(R)}$, (b) $\Delta E(\hat{\Phi}_{ex})/E_L$, and (c) p_L at $E_L/k_BT = 10$ as a function of $\hat{\Phi}_{ex}$.

with $\hat{\Phi}_{L(R)0}$ being the magnetic flux in an unbiased case. Note that the slope, a, can be controlled by changing β_L using the tunable Josephson junction[19–21].

The fitting line of the numerical results on $\Delta E_{num}/E_L$

is given by the relation,

$$\Delta E_{num}/E_L = 1.716\hat{\Phi}_{ex} - 0.858. \quad (21)$$

The approximate expression yielded the values $a = 1.856$ and $b = -0.858$. In spite of the poor approximation of the third order, the approximate expression is reasonably consistent with the numerical results. The calculations presented above clearly proves that the energy difference of the SQUID is linear to the external magnetic flux in practice. Therefore, flux-biased SQUIDs can be regarded as a highly operational sigmoid function using external magnetic flux as the input variable.

IV. CONCLUDING REMARKS

The stochastic transition between two states in a double well potential has been studied to show the physical basis of artificial neurons with the sigmoid function as the most suitable mathematical function for back propagation learning algorithm. We found that the transition probability is exactly described by the sigmoid function as a function of the energy difference between two states. It should be noted, however, that in order for the resulting sigmoid function to act as an activation function, the energy difference must be linear to the input variable in artificial neural networks. Upon using it to analyze the SQUID-based artificial neurons, we have derived the analytical expressions for its sigmoid functions. Finally, the transition model is applicable for any physical system with two states.

ACKNOWLEDGMENTS

We would like to thank S. Ishizaka for his helpful discussions and suggestions. This work is supported in part by MEXT(17K05579).

[1] F. Rosenblatt, *Principles of Neurodynamics: Perceptrons and the Theory of Brain Mechanisms* (Spartan Books, Washington, 1962).

[2] D. E. Rumelhart, G. E. Hinton, and R. J. Williams, "Learning representations by back-propagating errors," Nature **323**, 533–536 (1986).

[3] S. Sato, K. Nemoto, S. Akimoto, M. Kinjo, and K. Nakajima, "Implementation of a new neurochip using stochastic logic," IEEE Transactions on Neural Networks **14**, 1122–1127 (2003).

[4] S. Jung and S. s. Kim, "Hardware implementation of a real-time neural network controller with a dsp and an fpga for nonlinear systems," IEEE Transactions on Industrial Electronics **54**, 265–271 (2007).

[5] Y. Harada and E. Goto, "Artificial neural network circuits with josephson devices," IEEE Transactions on Magnetics **27**, 2863–2866 (1991).

[6] M. Hidaka and L. A. Akers, "An artificial neural cell implemented with superconducting circuits," Superconductor Science and Technology **4**, 654 (1991).

[7] Y. Mizugaki, K. Nakajima, Y. Sawada, and T. Yamashita, "Superconducting neural circuits using fluxon pulses," Applied Physics Letters **62**, 762–764 (1993), https://doi.org/10.1063/1.108571.

[8] Y. Mizugaki, K. Nakajima, Y. Sawada, and T. Yamashita, "Implementation of new superconducting neural circuits using coupled squids," IEEE Transactions on Applied Superconductivity **4**, 1–8 (1994).

[9] T. Onomi and K. Nakajima, "The use of artificial neural networks for classification of signal sources in cognitive radio systems," Programming and Computer Software **42**, 121 (2016).

[10] T. V. Filippov, Y. A. Polyakov, V. K. Semenov, and K. K. Likharev, "Signal resolution of rsfq comparators," IEEE Transactions on Applied Superconductivity **5**, 2240–2243 (1995).

[11] Y. Yamanashi, K. Umeda, and N. Yoshikawa, "Pseudo sigmoid function generator for a superconductive neural network," IEEE Transactions on Applied Superconductivity **23**, 1701004–1701004 (2013).

[12] A. E. Schegolev, N. V. Klenov, I. I. Soloviev, and M. V. Tereshonok, "Adiabatic superconducting cells for ultra-low-power artificial neural networks," Beilstein J Nanotechnol **7**, 1397–1403 (2016).

[13] P. Hänggi, P. Talkner, and M. Borkovec, "Reaction-rate theory: fifty years after kramers," Rev. Mod. Phys. **62**, 251–341 (1990).

[14] K. J. Laidler and M. C. King, "Development of transition-state theory," The Journal of Physical Chemistry **87**, 2657–2664 (1983), https://doi.org/10.1021/j100238a002.

[15] U. Weiss, *Quantum Dissipative Systems (4th Edition)* (World Scientific, 2012).

[16] A. D. H., H. G. E., and S. T. J., "A learning algorithm for boltzmann machines," Cognitive Science **9**, 147–169.

[17] H. Grabert, P. Olschowski, and U. Weiss, "Quantum decay rates for dissipative systems at finite temperatures," Phys. Rev. B **36**, 1931–1951 (1987).

[18] F. Chiarello, P. Carelli, M. G. Castellano, and G. Torrioli, "Artificial neural network based on squids: demonstration of network training and operation," Superconductor Science and Technology **26**, 125009 (2013).

[19] M. L. Schneider, C. A. Donnelly, S. E. Russek, B. Baek, M. R. Pufall, P. F. Hopkins, P. D. Dresselhaus, S. P. Benz, and W. H. Rippard, "Ultralow power artificial synapses using nanotextured magnetic josephson junctions," Science Advances **4** (2018), 10.1126/sciadv.1701329, http://advances.sciencemag.org/content/4/1/e1701329.full.pdf.

[20] I. P. Nevirkovets, S. E. Shafraniuk, O. Chernyashevskyy, D. T. Yohannes, O. A. Mukhanov, and J. B. Ketterson, "Investigation of current gain in superconducting-ferromagnetic transistors with high-j $_{rmc}$ acceptor," IEEE Transactions on Applied Superconductivity **27**, 1–4 (2017).

[21] I. I. Soloviev, N. V. Klenov, S. V. Bakurskiy, V. V. Bol'ginov, V. V. Ryazanov, M. Y. Kupriyanov, and A. A. Golubov, "Josephson magnetic rotary valve," Applied Physics Letters **105**, 242601 (2014), https://doi.org/10.1063/1.4904012.